HYDROGEN-ASSISTED FRACTURE IN FORGED TYPE 304L AUSTENITIC STAINLESS STEEL

N. SWITZNER

Kansas City Plant, managed by Honeywell Federal Manufacturing & Technologies LLC, Kansas City MO

J. HOLLENBECK

Kansas City Plant, managed by Honeywell Federal Manufacturing & Technologies LLC, Kansas City MO

W. EVERHART

Kansas City Plant, managed by Honeywell Federal Manufacturing & Technologies LLC, Kansas City MO

R. BERGEN

Precision Metal Products, El Cajon CA

C. SAN MARCHI

Sandia National Laboratories, Livermore CA

T. NEIDT

Kansas City Plant, managed by Honeywell Federal Manufacturing & Technologies LLC, Kansas City MO

J. KNUTSON

Kansas City Plant, managed by Honeywell Federal Manufacturing & Technologies LLC, Kansas City MO

R. HANLIN

University of Missouri-Kansas City, Kansas City MO

D.K. BALCH

Sandia National Laboratories, Livermore CA

ABSTRACT

Austenitic stainless steels generally have good resistance to hydrogen-assisted fracture; however, structural designs for high-pressure gaseous hydrogen are constrained by the low strength of this class of material. Forging is used to increase the low strength of austenitic stainless steels, thus improving the efficiency of structural designs. Hydrogen-assisted fracture, however, depends on microstructural details associated with manufacturing. In this study, hydrogen-assisted fracture of forged type 304L austenitic stainless steel is investigated. Microstructural variation in multi-step forged 304L was achieved by forging at different rates and temperatures, and by process annealing. High internal hydrogen content in forged type 304L austenitic stainless steel is achieved by thermal precharging in gaseous hydrogen and results in as much as 50% reduction of tensile ductility.

INTRODUCTION

Resistance to hydrogen-assisted fracture is an important consideration when selecting materials of construction for high-pressure gaseous hydrogen systems. Although austenitic stainless steels generally have good resistance to hydrogen-assisted fracture [1-4], structural designs with austenitic stainless steels are

constrained by the relatively low strength of this class of material. Forging and other thermomechanical processes can be used to increase the strength of austenitic stainless steels, thus improving the structural efficiency for applications that benefit from the use of high-strength materials, as in high-pressure systems. Hydrogen-assisted fracture, however, depends on both the intrinsic characteristics of a material as well as microstructural details from manufacturing the material or structure. Thus, it is important to understand the interplay between manufacturing processes, microstructural characteristics, and sensitivity to hydrogen-assisted fracture in materials of construction for service in high-pressure gaseous hydrogen.

In this study, the effect of internal hydrogen on tensile ductility of forged type 304L austenitic stainless steel was measured. High concentration of hydrogen (140 wt ppm) was precharged into the materials by exposure to high-pressure gaseous hydrogen at elevated temperature prior to testing. Microstructural variation in multi-step forged materials was achieved by forging at different rates and temperatures. Additionally, the effect of annealing prior to final forging was explored. The relationships between forging, microstructure and hydrogen-assisted fracture are discussed.

EXPERIMENTAL PROCEDURES

Details of the materials, forging processes, and testing in the as-forged condition are summarized in Ref. [5]. In brief, all forging was accomplished with material from the same starting bar of type 304L austenitic stainless steel (102 mm diameter, machined to 95 mm diameter prior to forging); the composition is given in Table 1. The forging rate and the temperature of the final forging step were varied in a three step forging process. The two initial extrusion steps (identical for all forgings) reduced the bar to 59 mm diameter. The final upset-forging step resulted in a forged cylinder with diameter of 71 mm. The rate of forging was varied by using different forging equipment for this final upset-forging step; in order of increasing deformation rate: (i) hydraulic press; (ii) mechanical press; (iii) screw press; and (iv) high energy rate forging (HERF). The temperature of the forging at the final step was also varied for each forging rate: the forgings were preheated to either 816 or 871°C. Additionally, the effect of annealing at a temperature of 954°C prior to the final forging step was also considered. Thus, forgings with 16 unique processing iterations were produced: four forging rates, each at two final-forging temperatures, and for each temperature, forged with and without a prior annealing step.

Tensile testing was conducted on cylindrical specimens taken axially at approximately the mid-radial position and approximately centered top-to-bottom in the forging. The gauge diameter was approximately 2.9 mm for all testing with a length between fillets of about 16 mm. Standard extensometry was used for measuring displacement on a gauge length of 12.7 mm. As-forged materials were tested at a constant crosshead displacement rate of 0.3 mm/min for the first 10% strain, then the displacement rate was increased to 2.5 mm/min until failure. The tensile testing results for the as-forged materials were previously reported in Ref. [6]. Tests on the hydrogen-precharged specimens were performed at constant crosshead rate of 0.3 mm/min until failure, which

corresponds to strain rate of approximately $4x10^{-4}$ s⁻¹. Replicate specimens were tested in the as-forged condition, single specimens were tested in the hydrogen-precharged condition. The 0.2% offset yield strength (Sy), ultimate tensile strength (Su), total elongation (Elt), and reduction of area (RA) are reported. The total elongation was determined from the digital tensile data when fracture occurs and the reduction of area was determined from the minimum diameter of the necked specimen measured after fracture with a knife-edged micrometer.

A uniform hydrogen concentration in the hydrogen-precharged specimens was achieved by long-time exposure to high-pressure gaseous hydrogen at elevated temperature, the so-called thermal hydrogen-precharging technique. Machined tensile specimens were placed in a high-pressure autoclave, which was then purged by evacuating and pressurizing (~20 MPa) with gaseous helium three times, followed by three cycles with high-purity gaseous hydrogen. The autoclave was then heated externally to temperature of 300°C and pressurized with gaseous hydrogen to a pressure of 138 MPa. The specimens were exposed to this environment for ~20 days to ensure uniform saturation through the full diameter of the specimens. These hydrogen-precharging conditions produce an equilibrium hydrogen content of about 140 wt ppm [2, 7], which was verified from several specimens after tensile testing. Additional details of the thermal preharging procedure can be found in Ref. [8].

RESULTS

The microstructure of all the forged materials is nominally the same. The ASTM grain size in the forged condition was 7 to 8 for all materials near the mid-radial location, and the grains were slightly elongated in the radial direction (due to upset/compression in the final forging step). Examples of the microstructure are given in Figure 1. A description of the subtle differences in microstructure are beyond the scope of this report; the interested reader is referred to Ref. [5].

The measured tensile properties are reported in Tables 2 and 3 for the two forging temperatures respectively. Materials forged at the higher temperature (871°C) showed a slightly lower yield strength by 5 to 10% compared to the same conditions except forged at the lower temperature (816°C); the ultimate tensile strength was also lower by about 5%. The total elongation was also slightly higher for the lower strength materials. The RA of the non-charged materials is a decreasing function of yield strength, within a tight range of 84 to 88%, as shown in Figure 2 (the yield strength of the non-charged material is used in these plots for the corresponding hydrogen-precharged condition to aid comparisons). Annealing prior to the final stage results in a slightly lower yield strength (typically about 2% reduction), but the effect of annealing is less than the effect of forging temperature; compare Figures 2a and 2b. The role of deformation rate is less systematic: the hydraulic process tends to result in the lowest yield strength, while the screw process produces the highest yield strength on average. There is, however, considerable overlap in the measured values of yield strength depending on the other processing parameters (Figure 2c). The effects of the prior anneal, strain rate, and temperature on the tensile properties of these (non-charged) materials are discussed in Ref [6].

Hydrogen-precharging increases the strength properties of these forgings by 10 to 20%, while the ductility parameters (Elt and RA) are reduced by typically 30 to 40% (but as much as 50%). The same basic trend is observed of decreasing RA as yield strength increases (Figure 2); however there tends to be more scatter of the RA in hydrogen-precharged materials with respect the basic trend and the slope of the overall trend is steeper by a factor of 2 to 3 (Figure 2c). In general, the loss in RA due to hydrogen is consistent for all the processing parameters. There appears, however, to be slightly greater sensitivity to hydrogen in the forgings that are annealed prior to the final forging step compared to those that have been not been annealed; compare the closed circles (non-annealed) to the closed triangles (annealed) in Figure 2b.

DISCUSSION

One of the intentions of this brief study was to determine if the deformation rate during forging of austenitic stainless steel results in any specific difference in hydrogen-assisted fracture. Materials for this study were obtained from prior work [5] that focused on the mechanical and microstructural properties as a function of the forging process. In the previous work, the deformation rate was not directly measured for these forging. Despite the fact that the deformation rate depends on a number of factors specific to a particular forging equipment and specific forging configuration, approximate values are known from the literature. Ref. [5] estimates deformation rates for these forging operations as 1, 5, 10 and 100 strain/s for hydraulic, mechanical, screw and HERF, respectively. While these variations in rates produce modest variation in strength and ductility parameters of the as-forged materials, these differences are relatively modest and there is overlap in the mechanical properties between the different forging proesses depending on other parameters such as forging temperature and prior annealing [6]. The ductility (RA) of the as-forged material, in particular, varies with the yield strength and appears to be effectively independent of the forging process (Figure 2c). Similarly the grain size is not significantly affected by the forging process and is relatively consistent for all the tested materials. The grain substructure, however, is dependent on the deformation rate, as reported in Ref. [5]. This observation of varying substructure suggested a possible difference in hydrogen-assisted fracture, since hydrogen-dislocation interactions are believed to play an important role in hydrogen-assisted fracture of austenitic stainless steels [9, 10].

Hydrogen-precharging produced a significant reduction in the RA for all the materials. The magnitude of the observed reduction is consistent with studies from the literature if the role of nickel content is considered. Figure 3 shows the RA of these tests compared to data from the literature for hydrogen-precharged type 304 and 316 alloys as a function of nickel content. The scatter in the data reported here is consistent with scatter from literature data and partially reflects the effect of strength. Additionally, the scatter here (particularly as evident in Figure 2) likely results from the lack of averaging that is achieved by replicate testing; the results for the as-forged condition, for example, represent an average of more than one test and show relatively little scatter (Figure 2).

While in general hydrogen resistance as measured by RA is not sensitive to the forging process and forging parameters, there appears to be a very subtle effect of prior annealing (Figure 2b). Annealing prior to the final stage of forging clearly reduces the strength of the forged material, which complicates comparison of hydrogen effects in forgings with and without annealing since the effect of strength is superimposed on the results. Nevertheless, the RA for hydrogen-precharged materials with prior annealing appears to follow a slightly lower trend than the RA for hydrogen-precharged material without prior annealing. Some of the accumulated strain energy associated with the first two forging steps is recovered during the annealing process; the temperature of the anneal is sufficiently low to prevent significant recrystallization [5]. Therefore, it is believed that there is more accumulated strain energy in forgings without prior annealing and consequently a higher dislocation density in the material.

The higher dislocation density may affect dislocation evolution during deformation; however, we speculate that the greater effect is on accumulation of dislocations in pile-ups. Since the higher dislocation density reduces the mean free path for dislocation motion and deformation in these materials tends to be characterized by the formation of slip bands, the number of dislocations in a slip band or dislocation pile-up will be less in materials with higher dislocation density. Fewer dislocations implies lower local stress and should result in higher ductility. This effect, if it exists, must be very small since there is no measurable effect of prior annealing on tensile ductility for the as-forged material. The dislocation mean free path, however, might be expected to be more important in the presence of hydrogen, since hydrogen interacts with dislocations and promotes localized deformation [11-13], thus the observed differences in hydrogen-precharged materials with and without annealing.

If the dislocation density is indeed sufficiently different due to prior annealing to manifest a difference in deformation and fracture in the presence of hydrogen, then tritium exposure may further amplify these differences. Tritium differs from hydrogen in that it decays to helium resulting in helium bubbles in stainless steels. The location of the helium bubbles in the microstructure is very important for the compatibility of the material and the distribution of helium depends (at least in part) on the dislocation structure. Thus partial recovery of the dislocation substructure due to the prior anneal could manifest as greater degradation due to tritium exposure than would be observed in material that is not recovered. Additional work is being pursued to address this question.

CONCLUSIONS

This paper explores the effects of forging parameters on hydrogen-assisted fracture in type 304L austenitic stainless steel by tensile testing of hydrogen-precharged specimens. Considering the same forging geometry and nominal deformation, the following conclusions can be drawn from this work:

- deformation rate does not significantly affect hydrogen-assisted fracture;
- forging temperatures of 816°C and 871°C do not significantly change the response of the material to high concentration of hydrogen; and
- in a multistage forging process, annealing prior to the final stage does not strongly affect hydrogen sensitivity, although this variable appears to be more important than the others explored in this study.

ACKNOWLEDGEMENTS

Sandia National Laboratories is a multi-program laboratory managed and operated by Sandia Corporation, a wholly owned subsidiary of Lockheed Martin Corporation, for the U.S. Department of Energy's National Nuclear Security Administration under contract DE-AC04-94AL85000.

REFERENCES

- GR Caskey. Hydrogen Compatibility Handbook for Stainless Steels (DP-1643). EI du Pont Nemours, Savannah River Laboratory, Aiken SC (June 1983).
- C San Marchi, BP Somerday, X Tang and GH Schiroky. Effects of alloy composition and strain hardening on tensile fracture of hydrogen-precharged type 316 stainless steels. Int J Hydrogen Energy 33 (2007) 889-904.
- 3. C San Marchi and BP Somerday. Technical Reference on Hydrogen Compatibility of Materials (SAND2008-1163). Sandia National Laboratories, Livermore CA (2008).
- 4. C San Marchi, T Michler, KA Nibur and BP Somerday. On the physical differences between tensile testing of type 304 and 316 austenitic stainless steels with internal hydrogen and in external hydrogen. Int J Hydrogen Energy 35 (2010) 9736-9745.
- NT Switzner. Comparison of forging processes for 304L stainless steel. Master of Science Thesis, Colorado School of Mines (2007).
- NT Switzner, CJ Van Tyne and MC Mataya. Effect of forging strain rate and deformation temperature on the mechanical properties of warm-worked 304L stainless steel. J Mater Processing Technol 210 (2010) 998-1007.
- C San Marchi, BP Somerday and SL Robinson. Permeability, Solubility and Diffusivity of Hydrogen Isotopes in Stainless Steels at High Gas Pressure. Int J Hydrogen Energy 32 (2007) 100-116.
- C San Marchi, DK Balch, K Nibur and BP Somerday. Effect of high-pressure hydrogen gas on fracture of austenitic steels. J Pressure Vessel Technol 130 (2008) 041401.
- C San Marchi, KA Nibur, DK Balch, BP Somerday, X Tang, GH Schiroky and T Michler. Hydrogen-assisted fracture of austenitic stainless steels. in: BP Somerday, P Sofronis and R Jones, editors. Effects of Hydrogen on Materials. Proceedings of the 2008 International Hydrogen Conference (Moran WY, 2008), Materials Park OH: ASM International (2009) p. 88-96
- 10. C San Marchi. Hydrogen embrittlement of austenitic stainless steels and their welds. in: RP Gangloff and BP Somerday, editors. Gaseous hydrogen embrittlement of materials in energy technologies. 1. Cambridge UK: Woodhead Publishing (2012) p. 592-623.
- 11. KA Nibur, DF Bahr and BP Somerday. Hydrogen effects on dislocation activity in austenitic stainless steel. Acta Mater 54 (2006) 2677-2684.
- C San Marchi, BP Somerday and HF Jackson. Hydrogen-assisted deformation and fracture of austenitic stainless steels. in: 2nd International Conference of Engineering Against Fracture (ICEAF II), 22-24 June 2011, Mykonos, Greece.
- KA Nibur, BP Somerday, DK Balch and C San Marchi. The role of localized deformation in hydrogen-assisted crack propagation in 21Cr-6Ni-9Mn stainless steel. Acta Mater 57 (2009) 3795-3809.

(a) (b)

Α

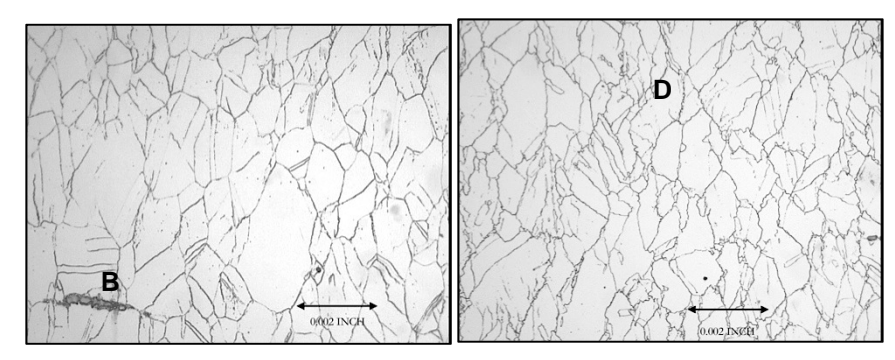


Figure 1. Metallographic images of forged 304L stainless steel: (a) material annealed at 954 °C, then mechanical press forged at 816 °C; and (b) material with no prior anneal, hydraulic press forged at 871 °C. Microstructural features include: (A) elongated grains from forging, (B) elongated ferrite from rolling, (C) bent annealing twins, and (D) "necklace" recrystallization beginning at the grain boundaries in the material forged at the higher temperature. Etched with 70/30 nitric acid at 1.1 volts.

Table 1. Composition of type 304L austenitic stainless steel used in this study.

		J /1							_
Fe	Cr	Ni	Mn	Si	C	N	S	P	
bal	19.48	10.69	1.63	0.52	0.029	0.03	0.0064	0.028	_

Table 2: Tensile properties of type 304L austenitic stainless steel, forged at temperature of 816°C.

temperature of 610 C.						
Process	Specimen	Condition	Sy (MPa)	Su (MPa)	Elt (%)	RA (%)
		non-charged	458	639	56	85
.RF	Annealed	H-precharged	530	734	42	43
HERF	Non-	non-charged	470	651	55	84
	annealed	H-precharged	555	760	35	43
	A 1.1	non-charged	483	642	57	85
≥	Annealed	H-precharged	557	738	27	44
screw	Non-	non-charged	495	656	55	85
	annealed	H-precharged	564	736	38	46
i	Annealed	non-charged	461	632	60	85
mech.	Annealed	H-precharged	530	730	45	46
Œ	Non-	non-charged	476	649	57	84
	annealed	H-precharged	533	742	45	50
. :	Annealed	non-charged	448	624	60	87
hvdr.	Annealed	H-precharged	510	723	51	48
h	Non-	non-charged	458	641	59	85
	annealed	H-precharged	521	725	47	57

Table 3: Tensile properties of type 304L austenitic stainless steel, forged at temperature of 871°C.

Dungaga	Cmaaiman	Condition	Sy	Su	Elt	RA
Process	Specimen		(MPa)	(MPa)	(%)	(%)

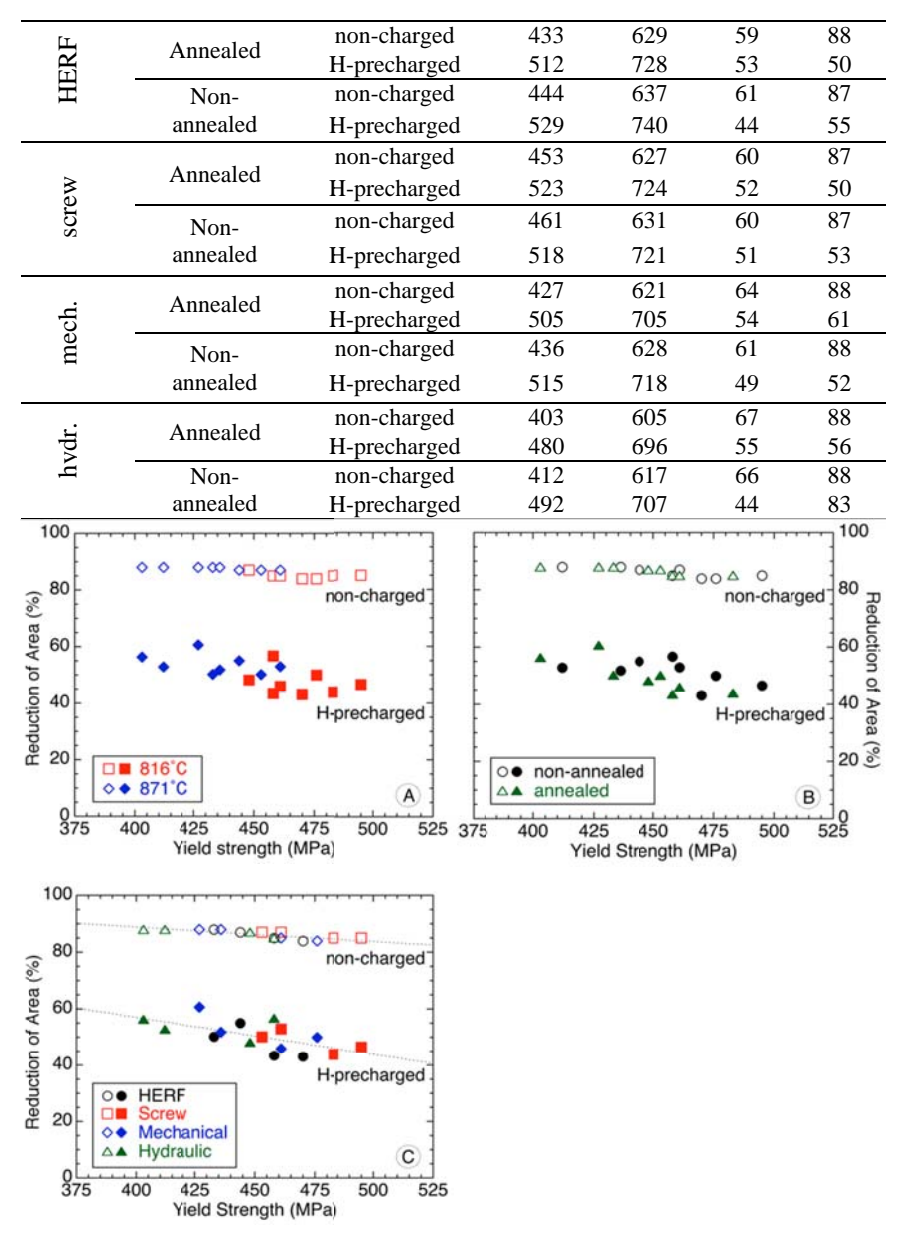


Figure 2. Tensile ductility as a function of yield strength for forged type 304L austenitic stainless steel: (a) effect of temperature; (b) effect of prior annealing; and (c) effect of deformation rate. Same data are plotted in each plot.

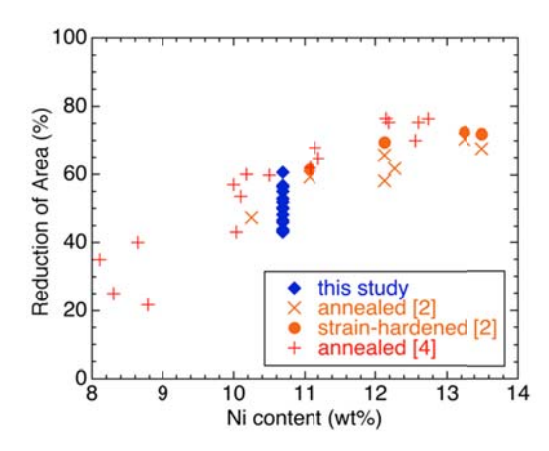


Figure 3. Tensile ductility as function of nickel content, comparing this study with data from the literature. The hydrogen concentration from Ref. [4](60 wt ppm) is substantially less than this study (140 wt ppm).